Vibration control of FGM plate using optimally placed piezoelectric patches

Z. Satla[a,b,c], L. Boumia[a,c], and M. Kherrab[c]

[a]*Ahmed Ben Yahia El Wancharissi university - Tissemsilt, BP 182, road de Bougara, Algeria,*
[b]*Laboratory of structural materials and solids, Sidi Bel Abbes, Algeria,*
[c]*Laboratory of Electronics, Computer Science and Applied Mathematics, Tissemsilt, Algeria.*

Received 11 April 2023; accepted 23 June 2023

The aim of this study is to propose a methodology to actively control the vibration of functionally graded plates, with the help of piezoelectric actuators and sensors. The study relays on the classical plate theory to analytically formulate the governing equation of motion, which is then expanded to derive a space state equation of the model. The material properties of the FG plate are assumed to vary along the thickness direction. In order to improve the damping effectiveness, the location of the piezoelectric sensors and actuators is optimally determined using the H2 norm. The necessary control voltage was determined based on optimal LQR and LQG controllers.

Keywords: Functionally graded material; piezoelectric; actuator; sensor; LQR controller.

DOI: https://doi.org/10.31349/RevMexFis.70.011002

1. Introduction

Active vibration control (AVC) has become an important area of research in recent years, with applications in various engineering fields, such as aerospace, automotive, civil, and mechanical engineering. AVC involves the use of sensors, actuators, and control systems to mitigate unwanted vibrations in structures. The use of smart materials, such as piezoelectric materials, has proven to be an effective approach to implement AVC systems.

Active vibration control of composite and functionally graded plates using piezoelectric patches has been a topic of extensive research due to their potential in mitigating unwanted vibrations and improving structural performance. Several studies have been conducted to investigate the vibration behavior and control of such plates under different loading conditions. These studies have explored various aspects of the problem such as the optimal placement of piezoelectric patches, the use of higher order shear deformation theory, the dispersion of waves and characteristic wave surfaces, and the bending and free vibration analysis of functionally graded plates.

Numerous studies have been conducted to investigate the use of piezoelectric materials for AVC. Authors in Refs. [1] and [2] proposed an optimal placement method for piezoelectric patches on composite plates and functionally graded beams, respectively. In Refs.[3] and [4] are studied surface waves and dispersion of waves in functionally graded piezoelectric plates. In Ref. [5] is proposed a first-order shear deformation theory for the analysis of functionally graded plates. In [6] is investigated nonlinear vibration of functionally graded plates under random excitation. Ref. [7] presents an exact solution for the free vibration of thin functionally graded rectangular plates.

Several researchers have also investigated the control strategies for piezoelectric-based AVC systems. Reference [8] provides a comprehensive review of vibration control of active structures. In [9] it is proposed an active robust control approach for the geometrically nonlinear vibration of FGM plates. Authors in Ref. [10] employed fuzzy logic controllers for the active vibration control of an FGM rectangular plate. In [11] were used genetic algorithms for the optimal shape control of functionally graded smart plates. In [12] was studied the vibration control of functionally graded material plates patched with piezoelectric actuators and sensors under constant electric charge. In Ref. [13] were investigated the nonlinear dynamic response and active vibration control of piezoelectric functionally graded plates.

In addition to the above research, various optimization techniques have been used to determine the optimal placement of piezoelectric patches for AVC. In Ref. [14] the authors proposed a computational scheme based on spatial H2 measures for optimal sensor/actuator placement of flexible structures. In Ref. [15] were used genetic algorithms to optimize the piezoelectric actuator configuration on a flexible fin for vibration control. Authors in Ref. [16] employed an optimization approach to determine the optimal placement of collocated piezoelectric actuators and sensors on a thin plate.

Numerous studies have investigated the use of piezoelectric materials for this purpose, with many focusing on optimal placement and control strategies. Notable contributions to the field include the the work in Ref. [17], where active vibration damping of smart composite beams was achieved through a system identification technique. The researchers utilized piezoelectric sensors and actuators to monitor and control the structural response of the beam, resulting in improved damping and reduced vibration levels. In another study presented in Ref. [18], the authors investigated the optimal placement and active vibration control of piezoelectric smart flexible cantilever plates. The study proposed an optimization algorithm to determine the optimal location of piezoelectric patches for active control of plate vibration.

The aforementioned studies demonstrate the potential of piezoelectric materials for AVC systems. However, there is still room for further research to improve the effectiveness and efficiency of these systems. The objective of this study is to investigate the use of piezoelectric materials for the active vibration control of structures and to determine the optimal placement of piezoelectric patches using optimization techniques.

In this paper, we review the state-of-the-art in piezoelectric-based AVC systems and present our approach to optimizing the placement of piezoelectric patches. The rest of the paper is organized as follows: Section 2 presents the mathematical models and control strategies for piezoelectric-based AVC systems. Section 3 describes the optimization techniques used to determine the optimal placement of piezoelectric patches. In Sec. 4, we present numerical results and discussions. Finally, conclusions are drawn in Sec. 5.

Overall, this study aims to contribute to the development of effective and efficient piezoelectric-based AVC systems for various engineering applications.

2. Fundamental equations

2.1. Functionally graded material equations

This work utilizes the simple power law function to describe the material properties of FG materials, which has been found to meet all the necessary criteria for this application. The material properties can be expressed using this function as follows:

$$E_{fgm}(z) = (E_c - E_m)\, V_c^{Rn} + E_m,$$
$$\rho_{fgm}(z) = (\rho_c - \rho_m)\, V_c^{Rn} + \rho_m,$$
$$V_c = \left(\frac{2z+h}{2h}\right)^{Rn}. \tag{1}$$

The material properties in question are Young's modulus ($E_{fgm}(z)$), mass density ($\rho_{fgm}(z)$), and the power law index (Rn). The subscripts "m" and "c" denote the metallic and ceramic constituents, respectively, while Vc represents the volume fraction of the ceramic. In Fig. 2, the relationship between the Young's modulus of the plate FGM and its non-dimensional thickness is plotted for various values of n.

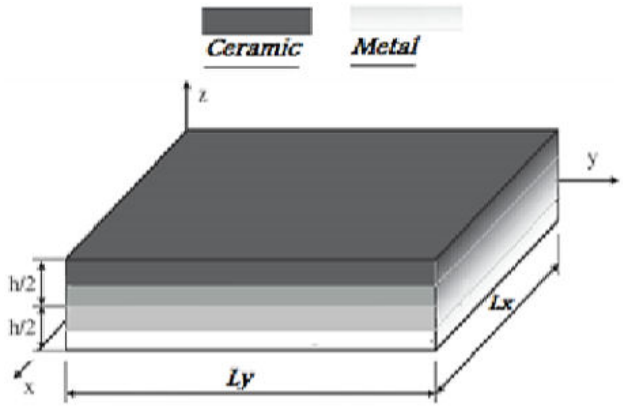

FIGURE 1. Model of the FGM plate and coordinate system.

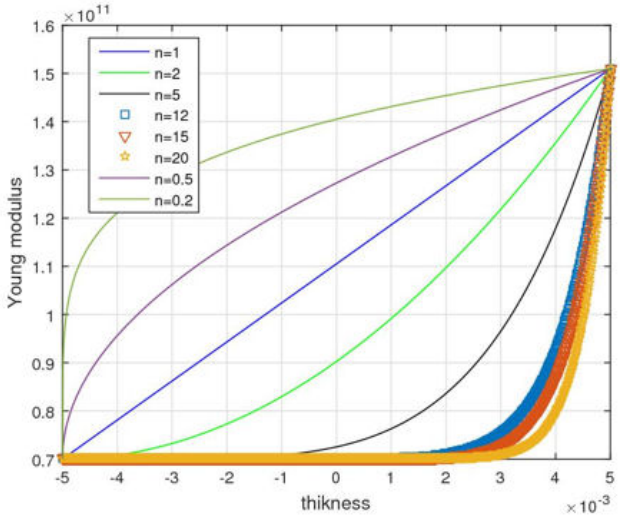

FIGURE 2. Variation of Young's modulus versus the plate thickness for different value of the index.

2.2. FGM plate equations

Based on the classical plate theory (CPT), the displacement components are assumed to be [19]:

$$u = u_0 - z\frac{\partial w_0}{\partial x}, \quad v = v_0 - z\frac{\partial w_0}{\partial y}, \quad w = w_0, \tag{2}$$

where u_0 and v_0: denote the displacement of mid-plane in x and y directions, respectively; w_0, the transverse displacement in the z direction. Using the strain-displacement relations, the strain components are defined as:

$$\varepsilon_{xx} = \frac{\partial u_0}{\partial x} - z\frac{\partial^2 w_0}{\partial x^2}, \quad \varepsilon_{yy} = \frac{\partial v_0}{\partial y} - z\frac{\partial^2 w_0}{\partial y^2},$$
$$\gamma_{xy} = \frac{\partial u_0}{\partial y} + \frac{\partial v_0}{\partial x} - 2z\frac{\partial^2 w_0}{\partial x \partial y}. \tag{3}$$

Based on the Hooke's law for FG rectangular plates in plane stress state, the stress-strain relations are expressed as:

$$\begin{pmatrix} \sigma_x \\ \sigma_y \\ \sigma_{xy} \end{pmatrix} = \begin{bmatrix} c_{11} & c_{12} & 0 \\ c_{21} & c_{22} & 0 \\ 0 & 0 & c_{66} \end{bmatrix} \begin{pmatrix} \varepsilon_x \\ \varepsilon_y \\ \varepsilon_{xy} \end{pmatrix}, \tag{4}$$

where $c_{11} = c_{22} = (E(z)/1 - v_{fgm}^2)$, $c_{12} = c_{21} = v_{fgm}^2 c_{11}$, $c_{66} = E(z)/2\,(1 + v_{fgm})$ σ_{ij} are the stress components, and ε_{ij} are the corresponding strains.

2.3. Piezoelectric constitutive equations

The coupling between the elastic field and the electric field may be described by the constitutive equations for the orthotropic piezoelectric material by the following Eqs. (5) and (6) [20].

$$\begin{Bmatrix} {\sigma_{xx}}^{pe} \\ {\sigma_{yy}}^{pe} \\ {\sigma_{xy}}^{pe} \end{Bmatrix} = \begin{bmatrix} Q^{pe} & Q^{pe} & 0 \\ Q^{pe} & Q^{pe} & 0 \\ 0 & 0 & Q^{pe} \end{bmatrix} \begin{pmatrix} \varepsilon_x \\ \varepsilon_y \\ \varepsilon_{xy} \end{pmatrix} - \begin{bmatrix} 0 & 0 & e_{31} \\ 0 & 0 & e_{32} \\ 0 & 0 & 0 \end{bmatrix} \begin{pmatrix} E_x \\ E_y \\ E_z \end{pmatrix}, \tag{5}$$

$$\begin{Bmatrix} {D_x}^{pe} \\ {D_y}^{pe} \\ {D_z}^{pe} \end{Bmatrix} = \begin{bmatrix} 0 & 0 & 0 \\ 0 & 0 & 0 \\ e_{31} & e_{32} & 0 \end{bmatrix} \begin{pmatrix} \varepsilon_x \\ \varepsilon_y \\ \varepsilon_{xy} \end{pmatrix} - \begin{bmatrix} \epsilon_{11} & 0 & 0 \\ 0 & \epsilon_{22} & 0 \\ 0 & 0 & \epsilon_{33} \end{bmatrix} \begin{pmatrix} E_x \\ E_y \\ E_z \end{pmatrix}, \tag{6}$$

where D represents the electric displacement components, E denotes the electric field component, Q, e and ϵ are the elastic, the piezoelectric coupling and the dielectric permittivity constants

2.4. Dynamic equations

According to the Hamilton principle, the dynamic, Eqs. (7a), (7b), and (7c), is given by

$$({M_{xx}}^{sp}, {M_{yy}}^{sp}, {M_{xy}}^{sp}) = \int_{-h/2}^{h/2} (\sigma_{xx} sp, {\sigma_{yy}}^{sp}, {\sigma_{xy}}^{sp})\, dz, \tag{7a}$$

$$\begin{Bmatrix} {N_{xx}}^{sp} \\ {N_{yy}}^{sp} \\ {N_{xysp}} \end{Bmatrix} = \int_{-h/2}^{h/2} \begin{Bmatrix} {\sigma_{xx}}^{p} \\ {\sigma_{yy}}^{p} \\ {\sigma_{xy}}^{p} \end{Bmatrix} dz + \int_{0}^{\frac{h}{2}+h_a} \begin{Bmatrix} \sigma_{xx}^{a} \\ \sigma_{yy}^{a} \\ \sigma_{xy}^{a} \end{Bmatrix} R dz + \int_{0}^{-\frac{h}{2}-h_s} \begin{Bmatrix} {\sigma_{xx}}^{s} \\ {\sigma_{yy}}^{s} \\ {\sigma_{xy}}^{s} \end{Bmatrix} R z dz, \tag{7b}$$

$$\begin{Bmatrix} {M_{xx}}^{sp} \\ {M_{yy}}^{sp} \\ {M_{xy}}^{sp} \end{Bmatrix} = \int_{h/2}^{-h/2} \begin{Bmatrix} {\sigma_{xx}}^{p} \\ {\sigma_{yy}}^{p} \\ {\sigma_{xy}}^{p} \end{Bmatrix} z dz + \int_{0}^{\frac{h}{2}+h_a} \begin{Bmatrix} \sigma_{xx}^{a} \\ \sigma_{yy}^{a} \\ {\sigma_{xy}}^{a} \end{Bmatrix} R dz + \int_{0}^{-\frac{h}{2}h_s} \begin{Bmatrix} {\sigma_{xx}}^{s} \\ {\sigma_{yy}}^{s} \\ {\sigma_{xy}}^{s} \end{Bmatrix} R z dz, \tag{7c}$$

where the subscripts p, a and s, represent the plate, actuator and sensor constituents respectively; R, represents the location function defined as:

$$R = \left[H\left(x - x_{1i}\right) - H\left(x - x_{2i}\right)\right]\left[H\left(y - y_{1i}\right) - H\left(y - y_{2i}\right)\right], \tag{8}$$

where H the Heaviside step function; (x_{1i}, y_{1i}) and (x_{2i}, y_{2i}), are the ith piezoelectric actuator coordinate.

Then, substituting Eq. (7) into Eq. (5), and by further simplification done by [12, 18], the equation of motion is obtained as:

$$\begin{aligned} D_i\left(\frac{\partial^4 w}{\partial x^4} + 2\frac{\partial^4 w}{\partial x^2 \partial y^2} + \frac{\partial^4 w}{\partial y^4}\right) + \bar{\rho} h \frac{\partial^2 w}{\partial t^2} = \sum_{i=1}^{Na} \Big\{ & C_0^i \varepsilon_{pe}^i \left[\delta'(x - x_{1i}) - \delta'\left(x - x_{2i}\right)\right]\left[H\left(y - y_{1i}\right) - H\left(y - y_{2i}\right)\right] \\ & + C_0^i \varepsilon_{pe}^i \left[\delta'(y - y_{1i}) - \delta'\left(y - y_{2i}\right)\right]\left[H\left(x - x_{1i}\right) - H\left(x - x_{2i}\right)\right] \\ & + 2C_0^i \varepsilon_{pe6}^i \left[\delta\left(x - x_{1i}\right) - \delta\left(x - x_{2i}\right)\right]\left[\delta\left(y - y_{1i}\right) - \delta(y - y_{2i})\right] \Big\}, \end{aligned} \tag{9}$$

where

$$\varepsilon_{pe}^i = \frac{d_{31i}}{h_{an}} V_i, \qquad \varepsilon_{pe6}^i = \frac{d_{36i}}{h_{an}} V_i, \qquad D_i = \int_{-h/2}^{h/2} \frac{-z^2 E(z)}{1 - v_{fgm}^2} dz, \qquad C_0^i = \frac{D_i (1 + v) p_n}{h_{an}},$$

$$P_n = \frac{12 E_p h_{an}(h_{an} + h)}{24 D_i (1 - V_p^2) + E_p[(h + 2h_{an})^3 - h^3]},$$

with N_a the actuators number, (x_{1i}, x_{2i}) and (y_{1i}, y_{2i}) are the locations of the ith piezoelectric actuator, $E_p, v_p, h_p, h_{an}, d_{31i}$, are the Young's modulus, the Poisson's ratio of the piezoelectric actuator, the half thickness of the plate, the piezoelectric actuator thickness, and the piezoelectric charge constant, respectively. plate, the piezoelectric actuator thickness, and the piezoelectric charge constant, respectively. the case of simply supported plate the solution of Eq. (9) is considered as:

$$W(x, y, t) = \sum_{i=1}^{\alpha} \phi_i(x, y) q(t), \tag{10}$$

with $\phi_i(x,y) = \sum_m \sum_n w_{mn} \sin(m\Pi/L_x) \sin(n\Pi/L_y)$ the mode shape of the simply supported plate; $q(t)$ the generalized coordinates for force function; L_x, L_y the length and width of the plate, respectively.

By introducing Eq. (10) in Eq. (9) and using the orthogonality properties of the FGM plate, the piezoelectric control equation can be written as a space state equation as follow:

$$\begin{aligned} \dot{X}(t) &= AX(t) + BU(t), \\ Y(t) &= Cx(t), \end{aligned} \tag{11}$$

with X the state at time (t), Y the output at time (t), A the state matrix, B the input matrix, and C the output matrix.

They are written as follows

$$\begin{aligned} A &= \begin{bmatrix} 0 & 1 \\ \Omega^2 & -2\zeta\Omega \end{bmatrix}, \quad B = C_0^i \begin{bmatrix} 0 \\ \psi_{mnr} \end{bmatrix}, \\ C &= \begin{bmatrix} 0 & \varphi \end{bmatrix}, \end{aligned} \tag{12}$$

with $\Omega = \text{diag}(\omega_{mn})$, $\zeta = \text{diag}(\xi_{mn})$, where ω_{mn} and ξ_{mn}, are the natural frequency and damping ratio of the n, m mode, respectively.

$$\begin{aligned} \psi_{mnr} = &\left[\frac{mL_a}{mL_a} + \frac{mL_b}{mL_b}\right] \left[\cos\left(\frac{n\pi y x_{1i}}{L_b}\right) - \cos\left(\frac{n\pi x_{2i}}{L_b}\right)\right] \\ &\times \left[\cos\left(\frac{n\pi y_{1i}}{L_b}\right) - \cos\left(\frac{n\pi y_{2i}}{L_b}\right)\right]. \end{aligned}$$

The index i represent the number of actuator.

2.5. Sensor equations

A piezoelectric (PZT) sensor is laminated on the FGM plate, the piezoelectric sensor generate an electric charge while the plate has some external stimulus. From Eq. (2) and Eq. (3), the output voltage of the ith piezoelectric sensor can be obtained as follows:

$$V^S(t) = \alpha \sum_{m=1}^{m=2} \sum_{n=1}^{n=2} \psi_{mnr} q(t), \tag{13}$$

where $\alpha = (k_{31}^2/g_{31})([h + h_{an}]/C_r)$. ψ_{mnr}, is the characteristic function, g_{31}, k_{31}, C_r. represent the voltage constant, the electromechanical coupling factor, and the PZT capacitance, respectively.

3. Control law

3.1. LQR optimal control

The idea beyond the LQR is to minimize a cost function given as [21]:

$$J = \int_0^\alpha (X^t Q X + U^t R U) dt = min, \tag{14}$$

where the matrices Q and R, are weighting matrices. It assumed that the desired state is $x = 0$, but the initial condition is non-zero, so the Q matrix penalizes the state error in a mean-square sense. Similarly, the R matrix penalizes the control effort, *i.e.*, limits the control signals magnitude. We design the optimal feedback control force U by the application of classical LQR control method,

$$U = K * x(t). \tag{15}$$

The gain matrix $K = R^{-1}B^T P$ which minimizes J can be found by solving a matrix Riccati equation given by:

$$PA + A^T P + Q - PBR^{-1}B^T P = 0. \tag{16}$$

3.2. LQG optimal control

In the previous equation it was assumed that all the states were completely observable and there could be directly related to the output and used by the control system. However, that is not always the case and a more realistic approach would consider that only the outputs can be known and measured, hence it will be necessary to estimate the states from a model of the system, usually that estimate is made by a state estimator or observer. Here we use Kalman-Bucy filter;.

$$\begin{aligned} X(t) &= AX(t) + BU(t) + B_w W(t), \\ Y(t) &= CX(t) + V(t), \end{aligned} \tag{17}$$

where $W(t)$ and $V(t)$ are modeled as white noise, featuring Gaussian stochastic processes with zero mean. It is considered that $W(t)$ and $V(t)$ are not correlated. The output vector are the system states, and the output matrix is an identity matrix.

$$W(t) = E[W(t)W^T(t)] = R_f \geq 0, \tag{18}$$

$$V(t) = E[V(t)V^T(t)] = Q_f > 0, \tag{19}$$

where E denotes the expectation operator. The estimator states would thus be governed by the equation,

$$\begin{aligned} \widehat{\dot{X}(t)} = &AX(t) + BU(t) \\ &+ K_e(t)[CX(t) + V(t) - C\widehat{X(t)}], \end{aligned} \tag{20}$$

where $K_e(t)$ is known as Kalman-Bucy filter given by:

$$K_e(t) = P_f C^T V^{-1}. \tag{21}$$

Defining the error between the true and estimated states as $e(t) = Xt) - \widehat{X(t)}$, we obtain

$$\begin{aligned} e(t) = &[A - K_e(t)C]e(t) \\ &+ BU(t) + W(t) - K_e(t)V(t), \end{aligned} \tag{22}$$

where P_f satisfies the algebraic Riccati equation:

$$P_f A^T + AP_f - P_f C^T V^{-1} C P_f + Q_f = 0. \tag{23}$$

3.3. Optimal placement of the piezoelectric patches

The actuators and sensors location have a major influence on the performance of the control system. Hence the placement of sensors and actuators must take in consideration of the observability and controllability. For this reason finding the best position of piezoelectric sensors and actuators has been the task of large number of researches [14, 16].In this section the optimal location of sensors and actuators are computed. The H2 norm developed by [18] is used to get the performance indices.

The H2 norm of the space state system Eq. (11) is define as:

$$\|G\|_2 = \sqrt{\left(\frac{1}{2\pi}\int_{-\infty}^{+\infty} \mathrm{tr}\left(G^*(\omega)G(\omega)\right) d\omega\right)}, \qquad (24)$$

where $G(\omega) = G_i(j\omega l - A_i)^{-1}B_i$, is the transfer function of the ith modes of the control system, *i.e.* can be also expressed as:

$$\|G_i\|_2 \cong \frac{\|B_i\|_2\|C_i\|_2}{2\sqrt{\zeta_i\omega_i}} \qquad (25)$$

Because the number of actuators is equal to that of the sensors, the modal H2 norm of jth input to the jth output is:

$$\|G_{ijj}\|_2 \cong \frac{\|B_{ij}\|_2\|C_{ij}\|_2}{2\sqrt{\zeta_i\omega_i}}, \qquad (26)$$

where B_{ij}, and C_{ij}, are the no-zero input and no-zero output matrices defined previously, for n inputs and outputs. By utilizing Eq. (26), the matrix norm is obtained. The placement index τ_{2ij} that evaluates the input and output for the ith modes is defined as:

$$\tau_{2ij} = \forall_i^j \|G_{ijj}\|_2, i = 1, ..., (m \times n), j = 1, ..., N_a, \quad (27)$$

where, $\forall_i^j \geq 0$ is the weight assigned to the jth actuator and the ith mode; N_a is the number of actuators,

$$\exists_2 = \begin{bmatrix} \tau_{2(11)1} & \cdots & \tau_{2(11)N_a} \\ \vdots & \ddots & \vdots \\ \tau_{2(mn)1} & \cdots & \tau_{2(mn)N_a} \end{bmatrix} i^{\text{th}} \text{ modes}, \qquad (28)$$

where the j^{th} column consists of indices of the j^{th} actuator for every mode, and the ith row is a set of the indices of the ith mode for all actuators. Now, the H2 norm optimal placement index for the actuator can be expressed as:

$$\text{Max} : \mu_{2aj} = \sqrt{\sum_{i=1X1}^{mXn} \tau_{2ij}^2}. \qquad (29)$$

Subject to:

$$\frac{l_p}{2} \leq x \leq L_x - \frac{l_p}{2}, \qquad \frac{b_p}{2} \leq x \leq L_y - \frac{b_p}{2},$$

where l_p and b_p are the length and the width of the piezoelectric patch, respectively; L_p and L_y: are the length and the width of the plate, respectively.

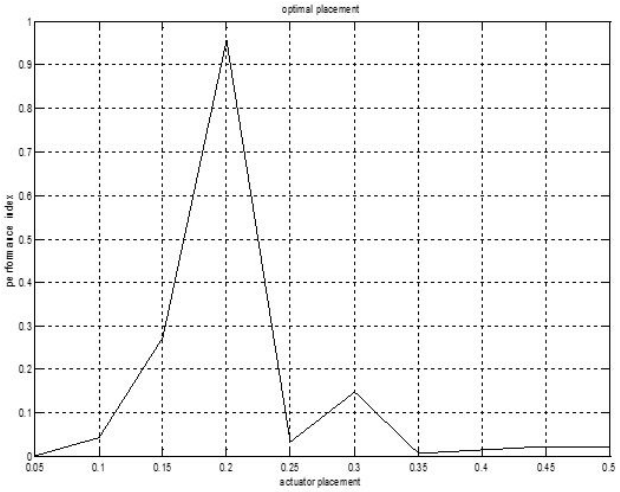

FIGURE 3. Actuator optimal placement.

4. Numerical examples and results

In this section we consider a simply supported FG plate bonded by six piezoelectric actuator patches on upper surfaces made of PZT G-1195 as shown in Fig. 3. For capturing the plate vibration two sensors were located in (0.3,0.2)m for sensor 1 and (0.2,0.3) for sensor 2. Plate dimensions are $500 \times 500 \times 10$ mm (Fig. 1). The principal material properties of FG plate are listed in Table I. Piezoelectric patches are of 70 mm length, 25 mm wide and 0.25 mm thickness in size. The parameters of the piezoelectric patches are also indicated in the same Table I.

TABLE I. Material properties of smart FGM plate [2].

Properties	Aluminum	Zirconium	PZT G-1195
Elastic modulus E (N/m^2)	70×10^9	151×10^9	6.3×10^{10}
Poisson's ratio	0.3	0.3	0.35
Density ρ (kg/m^3)	2702	7600	
Piezoelectric constant $d31$(m/V)	-	-	-1.66×10^{-10}
The electromechanical coupling factor $k31$	-	-	0.34
Voltage constant $g31$ (Vm/N)	-	-	-1.15×10^{-2}
Capacitance C(F)	-	-	1.05×10^{-7}

TABLE II. Natural frequencies for simply supported smart FGM plate with $n = 2$.

Mode (n, m)	1	2	3
1	569.9	1424.7	2849.5
2	0.3	2279.6	3704.3
3	0.3	3704.3	5129.0

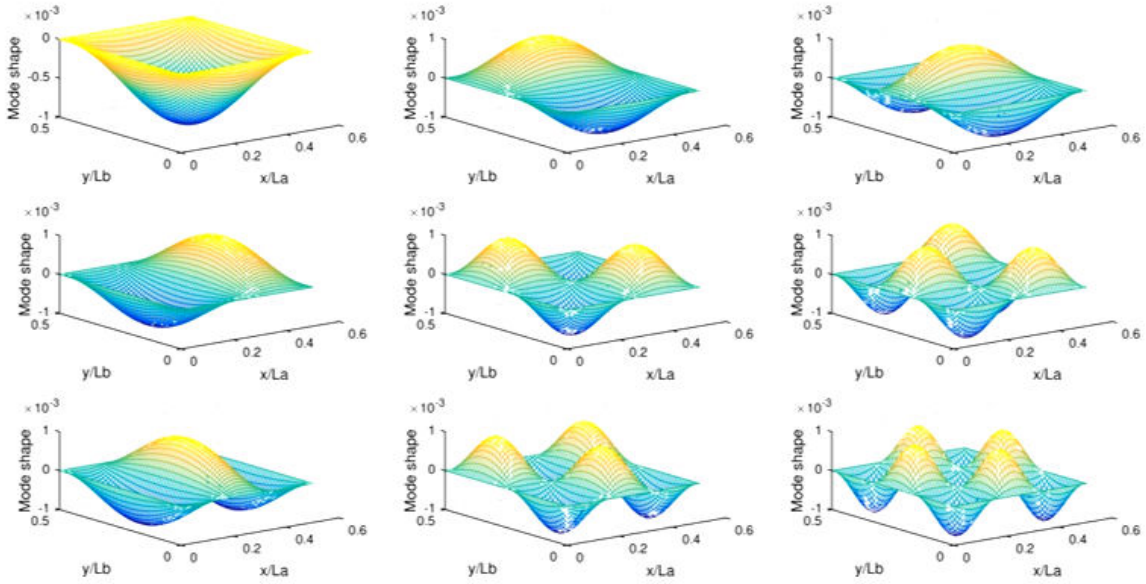

FIGURE 4. Modes shapes of the FGM plate.

Figure 5 shows the final decision of optimal placement of piezoelectric actuators on the FG plate. A decision of the first mode can be controlled efficiently. Of course, this is not the only best choice in all the cases. For example, the location of the actuators 1, 2 and 3 is nearest to the optimal location, because of the geometry limitation they cannot be located there, and the best choice may be taken in (0.2, 0, and 2).

Figure 6 shows the transient displacement response of the open loop comes from natural damping, while that of the closed loop system comes mainly from the feedback control with LQR controller and there of LQG controller. It can be observed that the LQG control has smaller stabilization time and oscillations amplitudes. However, the stabilization time, around 0.08 seconds for LQR and 0.04 seconds for LQG controller.

The control input driving by each actuator is presented in Fig. 7. It can be seen that the actuators five and six provide the maximum Input signal; however the maximum actuator voltage is larger in the case of LQR controller compared to that in the case of LQG control scheme. This clearly shows that the LQG control scheme leads to better control performance with less input voltages of actuators. The sensors output in close and open loop are present in Fig. 8 respectively.

The cost function as given by Eq. (14) is shown in Fig. 9 for the case of LQR controller, and in Fig. 10 for the case of LQG controller. The cost function depends up on control gains [20],

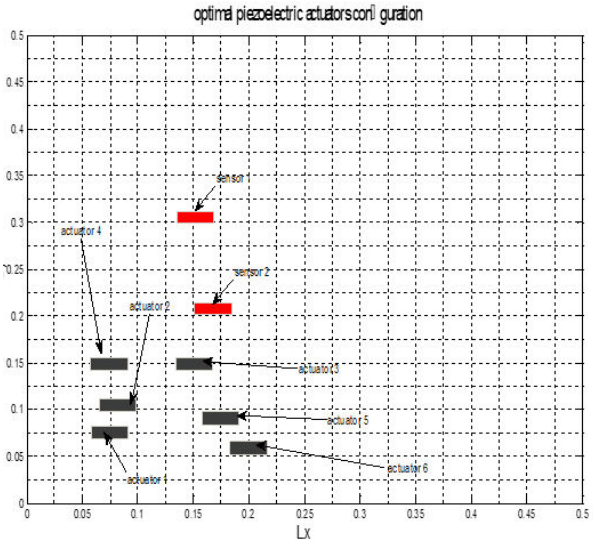

FIGURE 5. Optimal placement of piezoelectric actuators on the plate.

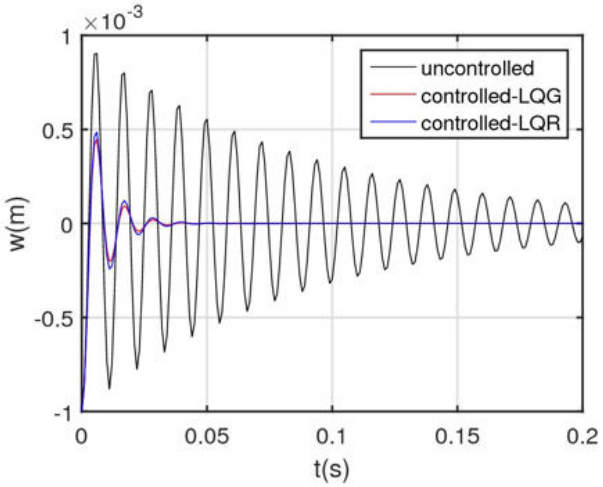

FIGURE 6. Vibration of the FGM plate amplitude with and without control.

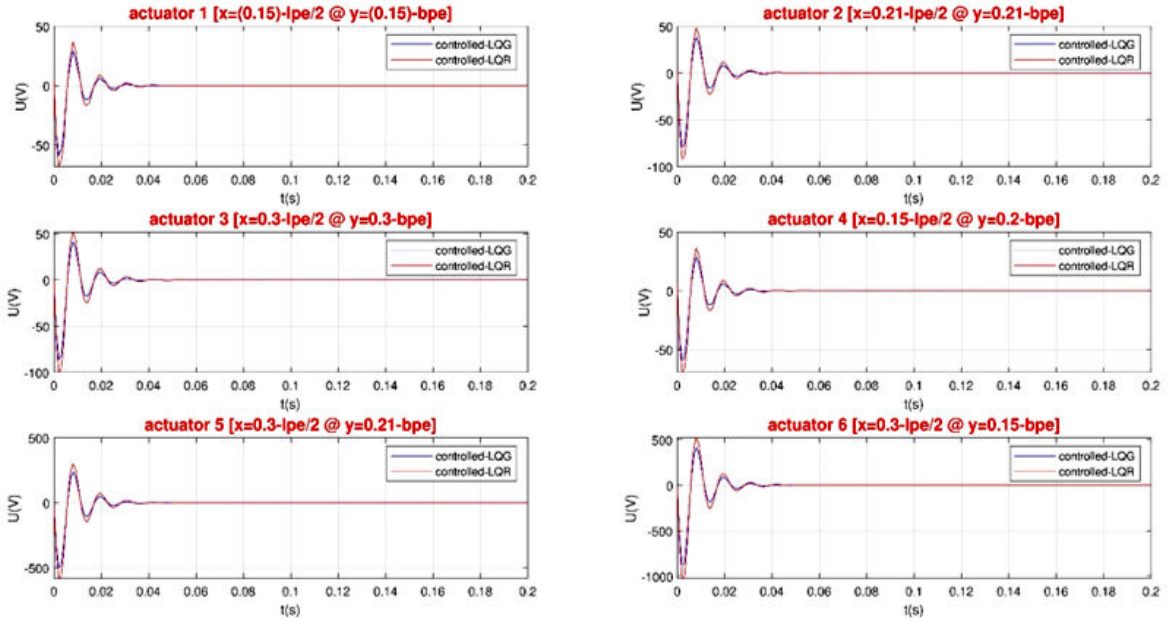

FIGURE 7. The input voltage corresponding to actuators 1, 2, 3, 4, 5 and 6.

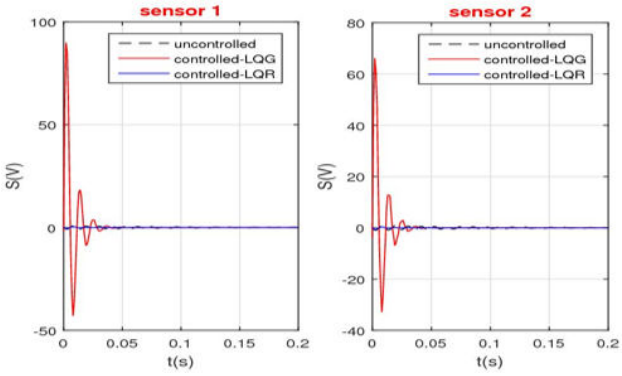

FIGURE 8. The output voltage corresponding to each sensor.

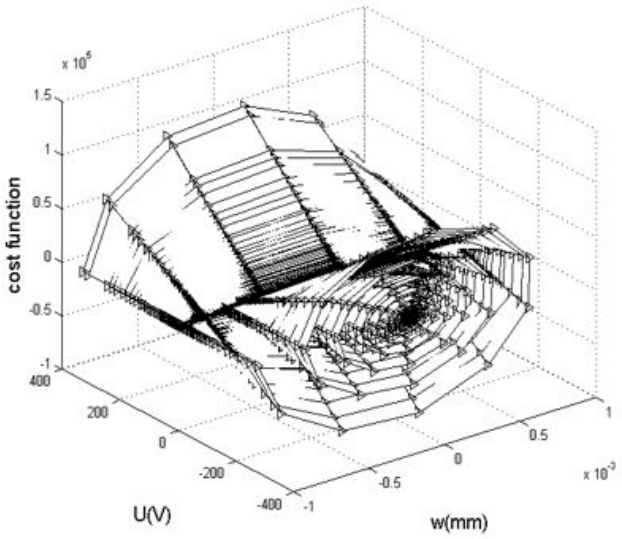

FIGURE 9. Cost function versus the displacement and the input voltage for the LQR controller.

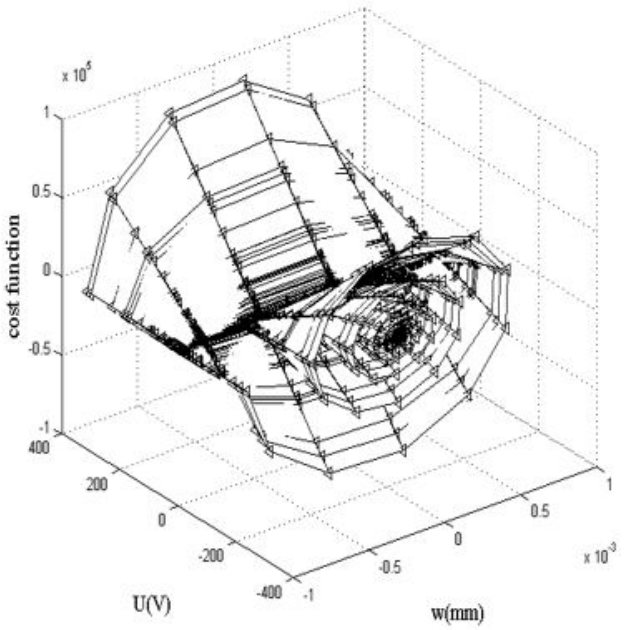

FIGURE 10. Cost function versus the displacement and the input voltage for the LQR controller.

the energy dissipated by the control system is maximized. In the LQG the energy is minimized much more than the case of LQR.

5. Conclusion

This paper investigates the optimal vibration control of a functionally graded material (FGM) plate using piezoelectric patches. The study presents various results that shed light on

the behavior of the plate and the effectiveness of using piezoelectric actuators and sensors for vibration control.

To analyze the behavior of the plate, the classical plate theory was employed. Spatial controllability and modal controllability concepts were then applied to identify the optimal placement of piezoelectric patches. The results obtained from finite element simulations showed that the location of the patches significantly affects the reduction of repair voltage magnitudes.

Furthermore, two optimal control strategies, namely linear quadratic regulator (LQR) and linear quadratic Gaussian (LQG) controllers, were developed and implemented to control the vibration of the plate. The LQR and LQG controllers were designed based on the modal controllability and system identification techniques, respectively.

The results of the study demonstrated that both controllers could stabilize the vibration of the plate, with a stabilization time of approximately 0.08 seconds for LQR and 0.04 seconds for LQG, and with a maximum voltage of 250 V for LQR and 220 V for LQG. It was observed that the LQG controller showed a better control bandwidth with lower control voltage compared to the LQR controller.

The study also investigated the maximum damping ratio, which was found to be around 0.06 for LQR and 0.08 for LQG. The obtained results showed the effectiveness of using piezoelectric patches for the optimal vibration control of FGM plates, and the importance of considering the location of patches and using appropriate control strategies.

Overall, this study provides valuable insights into the optimal vibration control of FGM plates, which can be beneficial in various engineering applications where vibration control is crucial.

1. K. Bendine *et al*., Active vibration control of composite plate with optimal placement of piezoelectric patches, *Mechanics of Advanced Materials and Structures* **26** (2019) 341, https://doi.org/10.1080/15376494.2017.1387324.
2. K. Bendine *et al*., Active vibration control of functionally graded beams with piezoelectric layers based on higher order shear deformation theory, *Earthquake Engineering and Engineering Vibration* **15** (2016) 611, https://doi.org/10.1007/s11803-016-0352-y.
3. G. R. Liu and J. Tani, Surface Waves in Functionally Gradient Piezoelectric Plates, *Journal of Vibration and Acoustics* **116** (1994) 440, https://doi.org/10.1115/1.2930447.
4. G. Liu *et al.*, Dispersion of waves and characteristic wave surfaces in functionally graded piezoelectric plates, *Journal of Sound and Vibration* **268** (2003) 131, https://doi.org/10.1016/S0022-460X(02)01494-3.
5. H.-T. Thai and D.-H. Choi, A simple first-order shear deformation theory for the bending and free vibration analysis of functionally graded plates, *Composite Structures* **101** (2013) 332, https://doi.org/10.1016/j.compstruct.2013.02.019.
6. V. Dogan, Nonlinear vibration of FGM plates under random excitation, *Composite Structures* **95** (2013) 366, https://doi.org/10.1016/j.compstruct.2012.07.024.
7. A. H. Baferani, A. R. Saidi, and E. Jomehzadeh, An exact solution for free vibration of thin functionally graded rectangular plates, Proceedings of the Institution of Mechanical Engineers, Part C: *Journal of Mechanical Engineering Science* **225** (2011) 526, https://doi.org/10.1243/09544062JMES2171.
8. A. Preumont, Vibration Control of Active Structures: An Introduction, Mathematics and Its Applicatio (Kluwer Academic Publishers, 1997), https://books.google.dz/books?id=afUeAQAAIAAJ.
9. V. Fakhari and A. Ohadi, Active robust control of geometrically nonlinear vibration of FGM plate with piezoelectric sensor/ actuator layers, *16th International Congress on Sound and Vibration* **3** (2009) 1472.
10. A. H. N. Shirazi, H. Owji, and M. Rafeeyan, Active Vibration Control of an FGM Rectangular Plate using Fuzzy Logic Controllers, *Procedia Engineering* **14** (2011) 3019, https://doi.org/10.1016/j.proeng.2011.07.380.
11. K. Liew, X. He, and S. Meguid, Optimal shape control of functionally graded smart plates using genetic algorithms, *Computational Mechanics* **33** (2004) 245, https://doi.org/10.1007/s00466-003-0525-1.
12. M. H. Kargarnovin, M. M. Najafizadeh, and N. S. Viliani, Vibration control of a functionally graded material plate patched with piezoelectric actuators and sensors under a constant electric charge, *Smart Materials and Structures* **16** (2007) 1252, https://doi.org/10.1088/0964-1726/16/4/037.
13. M. Yiqui and F. Yiming, Nonlinear dynamic response and active vibration control for piezoelectric functionally graded plate, *Journal of Sound and Vibration* **329** (2010) 2015, https://doi.org/10.1016/j.jsv.2010.01.005.
14. W. Liu, Z. Hou, and M. A. Demetriou, A computational scheme for the optimal sensor/actuator placement of flexible structures using spatial H2 measures, *Mechanical Systems and Signal Processing* **20** (2006) 881, https://doi.org/10.1016/j.ymssp.2005.08.030.
15. A. A. Rader *et al*., Optimization of Piezoelectric Actuator Configuration on a Flexible Fin for Vibration Control Using Genetic Algorithms, *Journal of Intelligent Material Systems and Structures* **18** (2007), https://doi.org/10.1177/1045389X06072400.
16. D. Halim and S. Reza Moheimani, An optimization approach to optimal placement of collocated piezoelectric actuators and sensors on a thin plate, *Mechatronics* **13** (2003) 27, https://doi.org/10.1016/S0957-4158(01)00079-4.

17. K. Bendine *et al.*, Active Vibration damping of Smart composite beams based on system identification technique, *Curved and Layered Structures* **5** (2018) 43, https://doi.org/10.1515/cls-2018-0004.

18. Z. cheng Qiu *et al*., Optimal placement and active vibration control for piezoelectric smart flexible cantilever plate, *Journal of Sound and Vibration* **301** (2007) 521, https://doi.org/10.1016/j.jsv.2006.10.018.

19. V. Birman, Plate structures, **vol. 178** (Springer Science & Business Media, 2011).

20. S. R. Moheimani and A. J. Fleming, Piezoelectric transducers for vibration control and damping, **vol. 1** (Springer, 2006).

21. K. Bendine *et al*., Structural modeling and active vibration control of smart FGM plate through ANSYS, International *Journal of Computational Methods* **14** (2017) 1750042.